ELSEVIER

Thin Solid Films 420–421 (2002) 345–349

thin solid films

www.elsevier.com/locate/tsf

# The technology for analyzing the conditions of rapid thermal annealing by optical second harmonic generation

Kuang-yao Lo[a,*], Ying-lang Wang[b], Jun-de Jin[c]

[a]*Department of Applied Physics, National Chia Yi University, Chia Yi 600, Taiwan, ROC*
[b]*Taiwan Semiconductor Manufacturing Company, Hsin-Chu 300, Taiwan, ROC*
[c]*Institute of Electronics Engineering, National TsingHua University, Hsin-Chu 600, Taiwan, ROC*

**Abstract**

Optical second harmonic generation (SHG) has been used to analyze the ULSI process, including low energy ion-implantation and rapid thermal annealing (RTA). The projected range of the low energy ion-implantation is approximately 20 nm, which results in a region that is transformed into an amorphous state by high dose ion-implantation, and the surface layer region is recrystallized during RTA process. The symmetrical point group of the Si (1 1 1) surface layer is 3 mm, which differs from that of centrosymmetric bulk Si which has no dipole contribution. The reflected SHG (RSHG) of the Si (1 1 1) is contributed mainly from the surface dipole and surface quadrupole. A plot of RSHG versus azimuthal angle reveals information on the recrystallization of amorphous silicon during RTA. The optimization of RTA step is determined by RSHG, which is shown to be suitable for analyzing the ULSI process.


*Keywords:* Second harmonic generation; Low energy ion-implantation; Rapid thermal annealing

## 1. Introduction

The efficiency of optical reflective second harmonic generation (RSHG) in light reflected from the surface of a solid has proven to be highly sensitive to the crystal lattice structure in the surface layer [1,2]. The symmetry of the second optical susceptibility that governs the process of second harmonic generation (SHG) is directly related to the lattice symmetry. The symmetry group of the silicon surface differs from that of the silicon bulk, which is a centrosymmetrical medium [3,4]. SHG is forbidden by the electric dipole within the centrosymmetrical medium. Therefore, in such materials the SHG signal is very strongly influenced by the surface layer in which the lowered symmetry enables the SHG process. Thus, the RSHG technique is a useful tool with which to probe the surface as well as the interface between two dense media.

At present, the line-width of the semiconductor devices extends to submicron scales. For very large scale integrated/ultra large scale integrated (VLSI/ULSI) fabrication processes, low energy ion-implantation with peak dopant concentrations depths of less than 50 nm, and rapid thermal annealing (RTA) are commonly employed to form shallow junctions. Characterization of the implant distribution is critically important for developing VLSI devices. RTA techniques have already been demonstrated for annealing the doped implanted layer to form shallow junctions [5]. In RTA processing, the temperature and the heating time are key to recrystallization in the dosed range and to diffuse the impurities over the desired range.

Secondary ion mass spectrometry is the most commonly used analytical technique for characterizing ion implants in semiconductors. While X-ray diffraction is frequently used to ensure the properties and the orientation of the crystal bulk. In addition, low energy electron diffraction (LEED) is commonly used to analyze the reconstructed surface. For the shallow dosed layer ($\sim$50 nm) due to low energy ion-implantation, the scale is too small to perform traditional X-ray diffraction analysis and too many atomic layers are present to effectively use LEED analysis. One promising

*Corresponding author. Tel.: +886-5-2717910; fax: +886-3-2717909.
*E-mail address:* kuanglo@mail.ncyu.edu (K.-y. Lo).

0040-6090/02/$ - see front matter © 2002 Elsevier Science B.V. All rights reserved.
PII: S0040-6090(02)00938-0

alternative is to use RSHG, since RSHG is sensitive to the crystal lattice structure of the surface layer, and the active region of RSHG is less than 100 nm using a pump laser wavelength of 1.064 μm.

RSHG is a new approach to gauging the recrystallized condition of the ion-implanted silicon during RTA for various temperatures and heating times. However, initial studies have shown that the RSHG technique is sufficiently sensitive to identify crystal variations, especially for the shallow layer, which is fabricated by low energy ion-implantation. This work presents the theory of this method, and an experiment to determine the best RTA condition via RSHG measurements.

## 2. Theory

The electrical dipole contribution is zero in a material such as silicon, with 3m-symmetry. In the surface region of silicon, the inversion symmetry of the bulk is broken and this greatly contributes to the non-linear polarization. A surface dipole term appears for a Si (1 1 1) surface with 3m-symmetry. SHG arises from the non-linear polarization $P(2\omega)$ induced by an incident laser field $E(\omega)$. For centrosymmetric media, the surface allowed dipole term can be written as

$$P_s(2\omega) = \chi^{(2)}_{s,ijk} E_j(\omega) E_k(\omega) \quad (1)$$

where $\chi^{(2)}_{s,ijk}$ is the second-order susceptibility tensor, reflecting the structure and symmetry properties of the surface layer. The $i$th component of the lowest-order bulk contributes to the non-linear polarization can be expressed as [6]

$$P_{B,i}(2\omega) = \gamma \nabla_i [E(\omega)E(\omega)] + \varsigma E_i(\omega) \nabla_i E_i(\omega) \quad (2)$$

where $\gamma$ and $\zeta$ are the only non-zero bulk terms and the $i$-directions are along the principal crystallographic axes. The first term gives rise to an isotropic contribution and the second term provides an anisotropic contribution that depends on the crystal symmetry.

For the case of a surface with 3m-symmetry, excited by s-polarized light, the s-polarized (or p-polarization) component of the radiated fields at 2ω is given by [7,8]

$$\begin{aligned} E_{s,s}(2\omega) &\sim (\chi_{\xi\xi\xi} - a\varsigma)\sin(3\varphi) \\ &\sim A_{s,s}\sin(3\varphi) E_{s,p}(2\omega) \\ &\sim (\chi_{\perp\parallel\parallel} - \gamma) - b\varsigma - c(\chi_{\xi\xi\xi} - a\varsigma)\cos(3\varphi) \\ &\sim B_{s,p} + C_{s,p}\cos(3\varphi) \end{aligned} \quad (3)$$

where $\varphi$ is the angle between the $x$-axis (parallel to $\langle 1\,1\,2\rangle$) and the plane of incidence, and $z$ is along the surface normal (Fig. 1). $\chi_{\xi\xi\xi}$ is the anisotropic and $\chi_{\perp\parallel\parallel}$ is the isotropic surface contribution; where $\perp$ and $\parallel$ indicate directions perpendicular and parallel to the surface, respectively; $\hat{\xi}$ is parallel to $\langle 1\,1\,\bar{2}\rangle$, and $a$, $b$ and $c$ are complex numbers that contain the Fresnel factors for reflection. Eq. (3) shows how bulk and surface terms appear in the same manner, such that they cannot be distinguished bulk term from surface term. Anyway, surface contribution dominates the RSHG intensity from the silicon surface because of the large absorption of silicon in the SHG wavelength of 532 nm. $A_{s,s}$ and $C_{s,p}$ reveal information regarding the crystal symmetry, since the RSHG intensity is dependent on the azimuthal angle. $B_{s,p}$ is an isotropic contribution which is dominated by the disorder strain in the crystal [9]. For low energy ion-implanted silicon, the surface is transformed into an amorphous state at a depth of 20 nm. The parameters $A_{s,s}$, $B_{s,p}$ and $C_{s,p}$ are the indexes of the crystalline condition, and thus indicate the variations in the surface layer among the various RTA treatments.

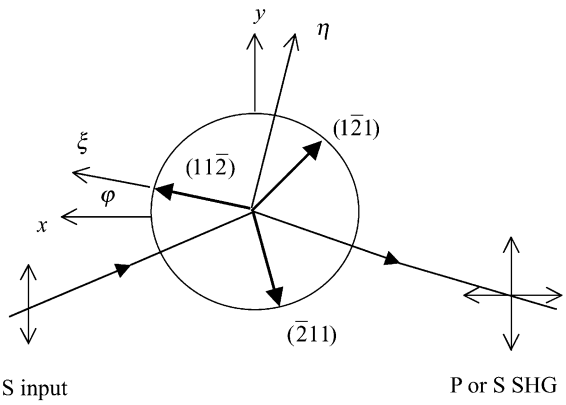


Fig. 1. Experimental geometry of the rotational anisotropy measurements. The rotation angle is defined as the angle between the lab frame $\hat{x}$-axis and the sample frame $\hat{\xi}$-axis.

## 3. Experimental procedures

### 3.1. Preparation of samples

The Si (1 1 1) samples implanted with $10^{16}$ cm$^{-2}$ As ions at an energy of 20 keV were studied. The projected range ($R_p$, the projection of this distance along the axis of incidence) of low energy implantation was 15.7 nm and the dose of the implant was sufficiently high to make the silicon surface amorphous over the projected range. The RTA process was carried out in a $N_2$ gas environment. Table 1 presents the heating temperatures, times evaluated in the present study.

The samples were standard, optically flat and polished Si (1 1 1) wafers with a native oxide. The oxide thickness was almost same for the samples following RTA, as it was before RTA treatment. The presence of the silicon oxide layer on the top of the samples did not appear to complicate the analysis of the results, since it was transparent and had a relatively low non-linearity yielding an imperceptible contribution to SHG [10].

Table 1
The conditions of RTA, and the corresponding RSHG factors

| Sample | Ion-implantation | RTA temperature | RTA time | $A_{s,s}$ | $B_{s,p}$ | $C_{s,p}$ | Sheet resistance ($\Omega/\square$) |
|---|---|---|---|---|---|---|---|
| Figs. 3 and 4a | No | No | No | 0.7829 | 0.1214 | 0.8670 | 20.75 |
| Figs. 3 and 4b | Yes | No | No | 0.3317 | 1.3463 | 0.0234 | – |
| Figs. 3 and 4c | Yes | 900 °C | 10 s | 0.4539 | 1.3357 | 0.0318 | 11.8 |
| Figs. 3 and 4d | Yes | 1000 °C | 10 s | 1.2973 | 0.3834 | 1.3819 | 8.21 |
| Figs. 3 and 4e | Yes | 1000 °C | 20 s | 1.2462 | 0.3820 | 1.3376 | 8.44 |
| Figs. 3 and 4f | Yes | 1100 °C | 10 s | 0.9138 | 1.2207 | 0.3246 | 8.28 |

The samples implanted with $10^{16}$ $cm^{-2}$ ions with energy of 20 keV.

### 3.2. Experimental methods

The laser source of the SHG experiment is a pulsed Q-switched Nd-Yag laser. The energy of the laser is up to 200 mJ per pulse and the duration of which is 6 ns. The laser spot was not highly focused to prevent damage to the Si samples, especially the amorphous one.

Fig. 2 shows the experimental setup. The laser beam was separated into two beams by the beam-splitter. The reference PMT tube measured the SHG signal generated from quartz, to monitor the laser's fluctuation and ensure the stability of the system. A concave lens and iris were positioned in front of the sample to adjust the size of the spot, and a blocking filter was also inserted to discard the 0.532 μm wavelength light generated by the above optical components. Before the PMT, there were an IR filter and a bandpass filter to obstruct 1.064 μm wavelength light and to percolate the SHG signal, respectively, and a polarizor to modulate the polarization of the RSHG. The RSHG signal from the sample was detected and recorded while the samples were stepwise rotated around their normal axis. The relative RSHG intensity was obtained by taking the ratio of the sample SHG intensity to the reference SHG intensity, in order to consider the stability of the laser and other factors in the system.

## 4. Results and discussion

For ease of comparison, all graphs of the experimental results are transformed into the polar coordinates, in which the radial dimension is the relative RSHG intensity and the angular dimension is the azimuthal angle. The scale of the radial dimension is the same in Fig. 3a–f and Fig. 4a–f, respectively.

Fig. 3a and Fig. 4a present s-polarized and p-polarized SHG intensity, respectively, from Si (1 1 1) without ion-implantation, as a reference. Fig. 3b–f and Fig. 4b–f depict s-polarized and p-polarized SHG intensity from Si (1 1 1), implanted with As ions at varied RTA temperatures and times. The corresponding RSHG factors ($A_{s,s}$, $B_{s,p}$ and $C_{s,p}$), listed in Table 1, were extracted by fitting the experimental results to Eq. (3). The sixfolds of s-polarization RSHG intensity is not clear when the RTA temperature is 900 °C (Fig. 3c), but becomes clear as the temperature increases and the amplitude of the folds reaches a maximum when temperature is 1000 °C at an annealing time of 10 s (Fig. 3d). However, the sixfolds of s-polarization RSHG intensity decreases as the annealing temperature increases to 1100 °C (Fig. 3f).

Following the above results, the pattern of p-polarization RSHG intensity is circular for the ion-implanted

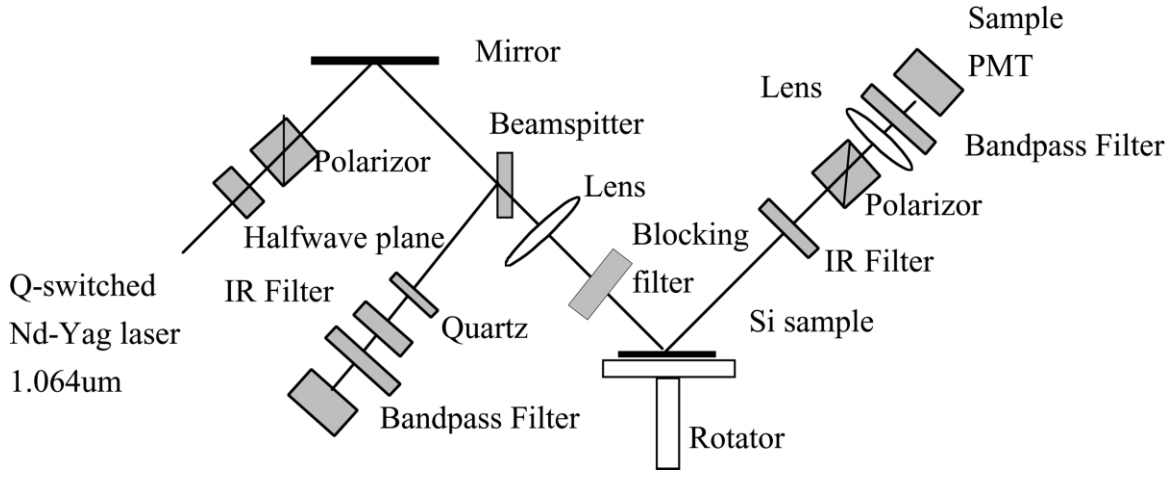


Fig. 2. Experimental setup.

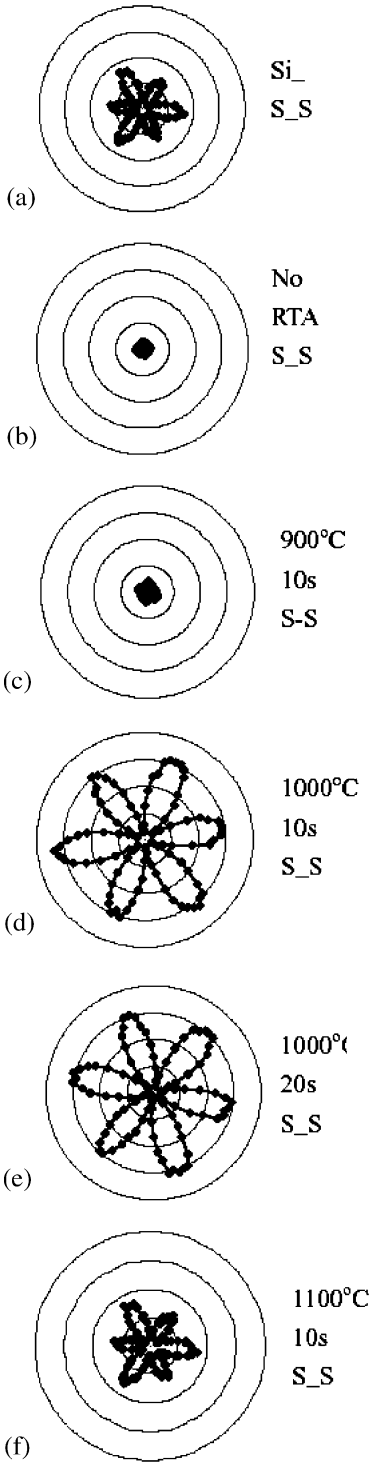


Fig. 3. S wave incident and S wave RSHG output for various RTA processes.

sample without RTA (Fig. 4b). The isotropic contribution ($B_{s,p}$) dominates the RSHG intensity because of the disordered structure of amorphous silicon; moreover, the RSHG intensity exceeds the silicon substrate due to the strong dipole contribution from the Si–As bond [11]. During RTA treatment the amorphous silicon is recrystallized, when the annealing temperature approaches 1000 °C (Fig. 4d). The anisotropic contribution ($C_{s,p}$) gradually becomes quite obvious because the surface layer exhibits a 3m-symmetric structure. When the annealing temperature is 1100 °C, the anisotropic term

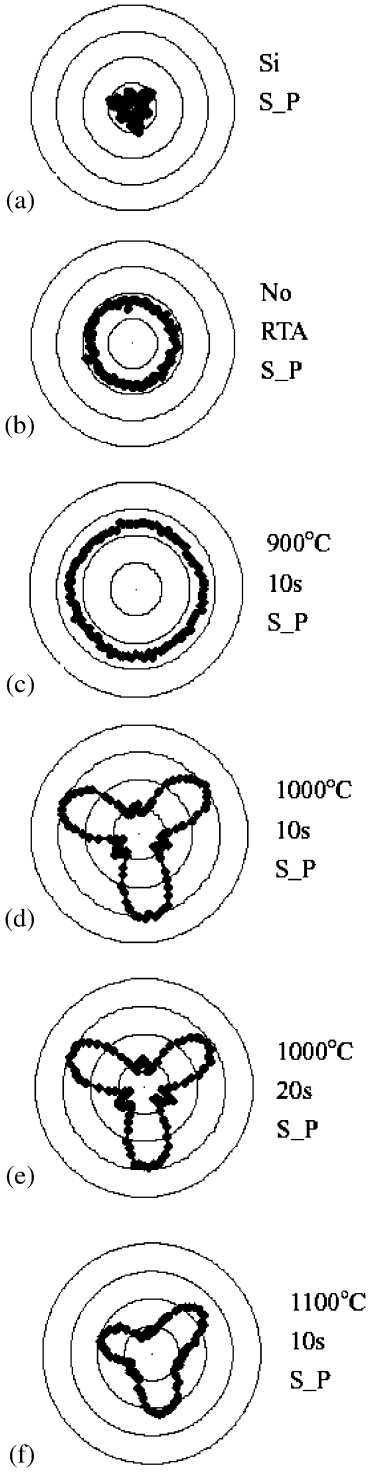


Fig. 4. S wave incident and P wave RSHG output for various RTA processes.

is lower than at 1000 °C. Arsenic atoms in the surface layer evaporate faster at higher temperatures and thus vacancy defects are left within the surface layer, enhancing the isotropic contribution, but weakening the anisotropic contribution which exhibits crystalline characteristics.

Fig. 3d–e and Fig. 4d–e compare samples at same annealing temperature, but different annealing times. Even though the diffusion length of an arsenic atom is larger at an annealing time of 20 s, the arsenic concentration of the near surface is less at this condition. Compare the parameters $A_{s,s}$, $B_{s,p}$ and $C_{s,p}$, listed in Table 1, the parameters of Fig. 3d and Fig. 4d are little larger than the ones of Fig. 3e and Fig. 4e. Since the RSHG is more sensitive beneath the surface layer, the parameters of RSHG reveal the informations of the surface more, including the surface structure and surface dipole contribution that impurity ions should enter the Si crystal lattice sites in a pattern of a well-ordered sublattice. The recrystallized quality of the silicon shallow layer is thus better with a shorter annealing time.

The sheet resistance of this sample was measured and following results were obtained (listed in the Table 1): 20.75 Ω/□ for Si (1 1 1) substrate, 11.8 Ω/□ for 10 s at 900 °C, 8.21 Ω/□ for 10 s at 1000 °C, 8.44 Ω/□ for 20 s at 1000 °C, and 8.28 Ω/□ for 10 s at 1100 °C. The least sheet resistance among the samples is 8.21 Ω/□ when the RTA temperature is 1000 °C and heating is limited to 10 s. Table 1 reveals that best annealing conditions correspond to larger $A_{s,s}$ and $C_{s,p}$, but smaller $B_{s,p}$ as such is the best condition for low sheet resistance. In the above discussion, the Si (1 1 1) substrate must be excluded because it was not treated with ion-implantation and RTA.

## 5. Conclusions

In conclusion, a comparative analysis of RSHG on the shallow layer of silicon was performed. A dependence of the pattern of RSHG intensity on the recrystalline condition was observed for a variety of RTA treatments. Optimized RTA conditions can be determined through RSHG analysis, since RSHG is sensitive to the variation of the very near surface region. RSHG is a sensitive tool for analyzing the quality of the thin film processing via ion-implantation and RTA post-treatment.

## Acknowledgments

The authors would like to thank the National Science Council (NSC) of the Republic of China (Taiwan) for financially supporting this research under Contract No. NSC 87-2112-M-168-001 and NSC 88-2112-M-168-001. The efforts of Professor Juh-Tzeng Lue at National Tsing Hua University is appreciated for their helpful discussions.

## References

[1] H.W.K. Tom, T.F. Heinz, Y.R. Shen, Phys. Rev. Lett. 51 (1983) 1983.
[2] C.V. Shank, R. Yen, C. Hirlimann, Phys. Rev. Lett. 51 (1983) 900.
[3] T.F. Heinz, M.M. Loy, W.A. Thomson, Phys. Rev. Lett. 54 (1985) 63.
[4] S.V. Govorkov, N.I. Koroteev, I.L. Shumay, Sov. Phys. Izv. 50 (1985) 683.
[5] T.E. Seidel, D.J. Lischner, C.S. Pai, R.V. Knoell, D.M. Maher, D.C. Jacobson, Nucl. Int. Methods Phys. Res. B 7/8 (1985) 251.
[6] C.W. van Hasselt, M.A. Verheijen, Th. Rasing, Phy. Rev. B 42 (1990) 9263.
[7] P.V. Kelly, J.D. O'Mahony, J.F. McGilp, Th. Rasing, Surf. Sci. 269/270 (1992) 849.
[8] J.E. Sipe, D.J. Moss, H.M. van Driel, Phys. Rev. B 35 (1987) 1129.
[9] C. Zhang, X. Xiao, N. Wang, K.K. Fung, M.M. Loy, Z. Chen, J. Zhou, Appl. Phys. Lett. 72 (1998) 2072.
[10] M.A. Veheijen, C.W. van Hasselt, Th. Rasing, Surf. Sci. 251/252 (1991) 467.
[11] S.V. Govorkov, V.I. Emel'yanov, N.I. Koroteev, G.I. Petrov, I.L. Shumay, V.V. Yakovlev, J. Opt. Soc. Am. B 6 (1989) 1117.